Fine Tuning [4 + 2] and [2 + 4] Diels−Alder Reactions Catalyzed by Lewis Acids

Shinichi Yamabe,*,† Tatsuo Dai,† and Tsutomu Minato‡

Contribution from the Department of Chemistry, Nara University of Education, Takabatake-cho, Nara, Nara 630, Japan, and Institute for Natural Science, Nara University, 1500 Misasagi-cho, Nara, Nara 631, Japan

Received April 26, 1994[⊗]

Abstract: Butadiene−acrolein Diels−Alder reactions with two kinds of Lewis acids, BF_3 and $AlCl_3$, were studied by using *ab initio* calculations. The transition-state structures of the cycloadditions with Lewis acids are quite asymmetric relative to that without Lewis acids. The transition state with BF_3 leads to an unexpected reverse-electron-demand cycloadduct, [2 + 4]. This adduct is transformed to a normal-electron-demand [4 + 2] product *via* a Cope rearrangement. For the $AlCl_3$ catalyzed reaction, the [4 + 2] or [2 + 4] selectivity is critical. Endo selectivity is ascribed to the coexistence of two competitive reaction paths.

I. Introduction

Lewis acid catalysis can have a significant effect on the rates and endo selectivities of Diels−Alder reactions.[1] When the Lewis acid is coordinated to a heteroatom, such as carbonyl oxygen, the endo selectivity is enhanced and rate acceleration is observed. The frontier molecular-orbital theory (FMO) explains the enhancement in terms of the change in the LUMO shapes of dienophiles.[2]

Diels−Alder reactions of substituted dienes and/or dienophiles have been extensively studied by means of theoretical calculations.[3] However, reports dealing with the reactions with Lewis acids are rather few, and they have been examined only qualitatively.[4] Birney and Houk[5] obtained four transition-state (TS) structures for a Diels−Alder reaction between butadiene and BH_3-coordinated acrolein. Their calculations reproduced well the effect of the Lewis acid catalysis, *i.e.*, decreased activation energies and enhanced endo selectivity. Of the four, the transition state (endo, acrolein with the s-cis conformation) was found to be the most stable. Unfortunately, this transition state was not located precisely. There seems to be a driving force for endo selectivity in this structure.

In this work, two commonly-used Lewis acids, boron trifluoride (BF_3) and aluminium trichloride ($AlCl_3$), were employed to describe the catalyzed acrolein−butadiene Diels−Alder reaction. We employed *s-cis*-acrolein as a dienophile. The effects of Lewis acids on the cycloaddition paths were investigated by *ab initio* calculations. It will be demonstrated that the BF_3-containing reaction leads to an unexpected cycloadduct, vinyldihydropyran rather than cyclohexene carboxaldehyde.

Scheme 1

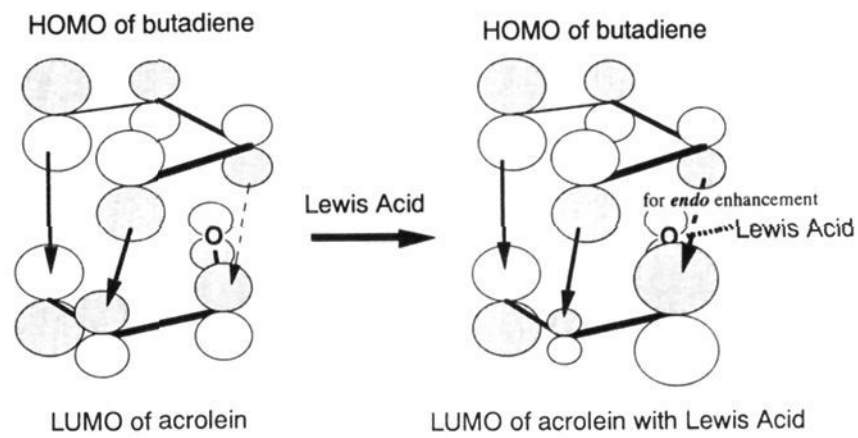

II. Method of Calculations

Ab initio calculations have been performed using the GAUSSIAN 92 program package[6] installed both on a CONVEX C-220 in the Information Processing Center of Nara University of Education and on a CONVEX C-3420 in the Computer Center of Nara University.

The 3-21G and 6-31G* basis sets were used for geometry optimizations. The transition-state geometries of the butadiene−acrolein system without any Lewis acids were optimized with four methods, RHF/3-21G, RHF/6-31G*, MP2/6-31G*, and CASSCF(8,8)/3-21G. For this CASSCF/3-21G calculation, the number of active space orbitals was selected on the basis of the occupation numbers of the natural orbitals obtained by a UHF calculation, CAS-UNO. At the RHF/3-21G transition-state geometry, occupation numbers of natural orbitals are 1.9986 (the 25th), 1.9986 (the 26th), 1.9657 (the 27th), 1.9376 (the 28th), 1.8577 (the 29th), 1.7143 (the 30th), 0.2858 (the 31st), 0.1423 (the 32nd), 0.0621 (the 33rd), 0.0343 (the 34th), 0.0014 (the 35th), and 0.0014 (the36th), where HOMO is the 30th MO. Thus, the active space orbitals adopted here were the MOs from the 27th to the 34th, and then CASSCF(UNO,8,8) led to 1764 configurations. A splicing basis set has been applied to systems with Lewis acid. This basis set is composed of the 6-31G* basis sets for butadiene and acrolein and the 3-21G basis set for Lewis acid (RHF/6-31G* & 3-21G).

† Nara University of Education.

‡ Nara University.

⊗ Abstract published in *Advance ACS Abstracts,* October 15, 1995.

(1) (a) Yates, P.; Eaton, P. *J. Am. Chem. Soc.* **1960**, *82*, 4436. (b) Inukai, T.; Kojima, T. *J. Org. Chem.* **1971**, *36*, 924.

(2) Fleming, I. *Frontier Orbitals and Organic Chemical Reactions*; Wiley: New York, 1976; Chapter 4.

(3) (a) Fox, M. A.; Cardona R.; Kiwiet, N. J. *J. Org. Chem.* **1987**, *52*, 1469. (b) Houk, K. N.; Loncharich R. J.; Blake, J. F.; Jorgensen, W. L. *J. Am. Chem. Soc.* **1989**, *111*, 9172. (c) Loncharich, R. J.; Brown, F. K.; Houk, K. N. *J. Org. Chem.* **1989**, *54*, 1129. (d) Gonzalez, J.; Houk, K. N. *J. Org. Chem.* **1992**, *57*, 3031. (e) McCarrick, M. A.; Wu Y.-D.; Houk, K. N. *J. Org. Chem.* **1993**, *58*, 3330. (f) Jorgensen, W. L.; Lim, D.; Blake, J. F. *J. Am. Chem. Soc.* **1993**, *115*, 2936.

(4) (a) Guner, O. F.; Ottenbrite, R. M.; Shillady, D. D.; Alston, P. V. *J. Org. Chem.* **1987**, *52*, 391 and references cited therein. (b) Sato, K.; Sakuma, Y.; Iwabuchi, S.; Hirai, H. *J. Polym. Sci., Part A: Polym. Chem.* **1992**, *30*, 2011.

(5) Birney, D. M.; Houk, K. N. *J. Am. Chem. Soc.* **1990**, *112*, 4127.

(6) Frisch, M. J.; Trucks, G. W.; Head-Gordon, M.; Gill, P. M. W.; Wong, M. W.; Foresman, J. B.; Johnson, B. G.; Schlegel, H. B.; Robb, M. A.; Replogle, E. S.; Gomperts, R.; Andres, J. L.; Raghavachari, K.; Binkley, J. S.; Gonzalez, C.; Martin, R. L.; Fox, D. J.; DeFrees, D. J.; Baker, J.; Stewart, J. J. P.; Pople, J. A.; *GAUSSIAN 92*, Revision C; Gaussian Inc.: Pittsburgh, PA, 1992.

0002-7863/95/1517-10994$09.00/0 © 1995 American Chemical Society

$\nu^{\ddagger}$(cm^{-1})	Ea [or ΔE] (kcal/mol)		$\nu^{\ddagger}$(cm^{-1})	Ea [or ΔE] (kcal/mol)
734.1i	27.08	RHF/3-21G	724.0i	27.03
(811.8i)	(36.04)	(RHF/6-31G*)	(803.8i)	(35.86)
447.2i	6.95	MP2/6-31G*	422.3i	5.69
	[0.24]	[CASSCF(8,8)/3-21G]		[0]
	17.52	MP3/6-31G*//RHF/3-21G		16.80

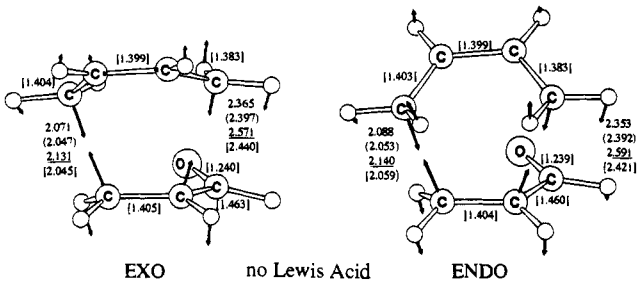

Figure 1. Transition-state structures of the Diels–Alder reaction without Lewis acids computed with various methods. Empty circles stand for hydrogen atoms. Distances are in Å. Intramolecular distances of C–C and C–O bonds are from the CASSCF(8,8)/3-21G method. $\nu^{\ddagger}$'s denote sole imaginary frequencies in cm^{-1} indicating that the obtained geometry is really of transition state. Their corresponding reaction-coordinate vectors are also sketched. *E*a's are the computed activation energies, and ΔE's are exo–endo energy differences (endo, more stable) in kcal/mol calculated by the CASSCF(8,8)/3-21G method.

Intrinsic reaction coordinates (IRC's)[7] starting from all the transition states obtained here were calculated to find energy-minimum points (reactants, products, or intermediates). Potential-energy diagrams were drawn from the results of the single-point calculations of the third-order Møller–Plesset perturbation wave function with the 6-31G* basis set on RHF/3-21G geometries, MP3/6-31G*//RHF/3-21G. Use of the MP3/6-31G* method is known to reproduce activation energies well.[3f]

III. Results of Calculations and Discussions

First, the Diels–Alder reaction without any Lewis acids was examined. The transition-state geometry of this system already has been examined at the Hartree–Fock level.[3c] Figure 1 shows the transition-state geometries of the acid-free reaction optimized by four methods. They are nearly insensitive to computational methods. The reaction-coordinate vector indicates that this reaction is concerted and formation of two bonds is almost synchronous. The four methods give quite small differences between exo- and endo-activation energies (E_a's), ~1 kcal/mol or less. The activation energy calculated here is close to an experimental value, 19.7 kcal/mol,[8] with *s-trans*-acrolein. Based on the similarity of the transition-state structures between RHF/3-21G and 1764-configuration MCSCF methods, we have determined the acid-catalyzed transition-state structures by RHF/3-21G and RHF/6-31G* methods.

Figure 2 exhibits EXO and ENDO transition-state geometries including BF_3. Differences in E_a values (ΔE_a's) between EXO and ENDO calculated here are larger than those without Lewis acid, which demonstrates that endo selectivity is enhanced by BF_3. As shown by Birney and Houk,[5] the formation of two bonds is significantly asynchronous in the transition-state geometries. In both EXO and ENDO, reaction-coordinate vectors indicate mainly the terminal (left-side) C···C bond formation. This asynchronous characteristic is also explicable in terms of the orbital interaction in Scheme 1. One curious vector component is found in the ENDO transition state. The component indicates a C···O bond formation (2.635 Å) instead of C···C (3.119 Å). That is, a reverse-electron demand

$\nu^{\ddagger}$(cm^{-1})	Ea (kcal/mol)		$\nu^{\ddagger}$(cm^{-1})	Ea (kcal/mol)
411.2i	9.88	RHF/3-21G	462.8i	7.95
(509.2i)	(17.22)	(RHF/6-31G* & 3-21G)	(568.8i)	(17.43)
	10.87	MP3/6-31G*//RHF/3-21G		6.09

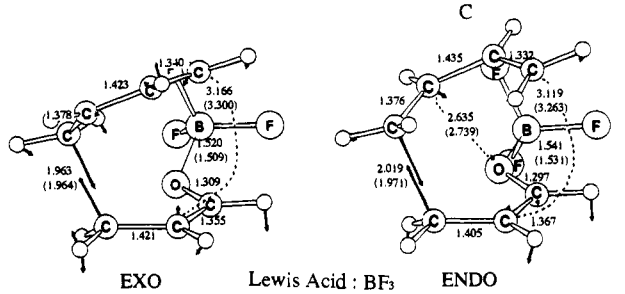

Figure 2. Transition-state structures of the Diels–Alder reaction with boron trifluoride. "6-31G* & 3-21G" is a splicing basis set, where butadiene and acrolein parts are from 6-31G* and the BF_3 part is from 3-21G. Other notations are the same as those in Figure 1. An unreasonable result of activation energies, 17.22 kcal/mol in EXO and 17.43 kcal/mol in ENDO, has been obtained with RHF/6-31G* & 3-21G. The reason of this result (probably, imbalance of two basis sets) is not clear at the present time. The large capital C attached to ENDO will be used in Figure 6 and Scheme 2.

$\nu^{\ddagger}$(cm^{-1})	Ea (kcal/mol)		$\nu^{\ddagger}$(cm^{-1})	Ea (kcal/mol)
399.3i	6.42	RHF/3-21G	403.1i	2.63
(502.4i)	(14.76)	(RHF/6-31G* & 3-21G)	(524.1i)	(11.84)
	6.15	MP3/6-31G*//RHF/3-21G		2.64

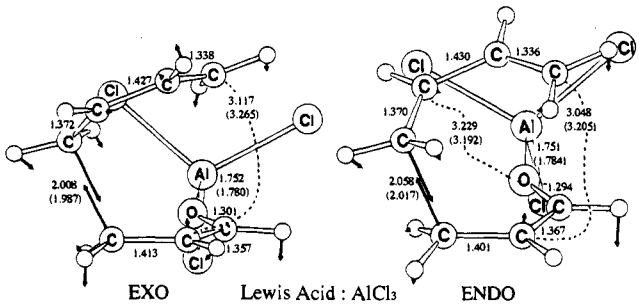

Figure 3. Transition-state structures of the Diels–Alder reaction with aluminium trichloride.

transition state, the [2 + 4] transition state, is suggested, rather than the normal one, the [4 + 2] transition state.[9]

Figure 3 shows EXO and ENDO transition-state geometries with $AlCl_3$. The left-side C···C bond in EXO or ENDO is ~2.0 Å, which is almost the same as that with BF_3. One cannot predict clearly whether the ENDO transition state is directed to a [4 + 2] adduct or to a [2 + 4] adduct because of the long C···C and C···O bond distances, 3.0~3.2 Å, in this transition-state structure.

In order to reveal cycloadducts after the transition states in Figures 2 and 3, we have performed IRC[7] calculations. The calculation shows the presence of novel π–π stacking charge-transfer complexes between butadiene and Lewis acid-coordinated acrolein at initial stages of the cycloadditions. Figure 4 shows those complexes. It is noteworthy that distances (3.8~4.0 Å) for the C···C bonds primarily formed at the transition states are larger than the other C···C bond distances (3.52~3.67 Å). At initial stages of the additions, the black-lobe overlap is more important than the white-lobe one (left-side) in Scheme 1.

The cycloadduct with BF_3 obtained at the other end of the IRC was not a [4 + 2] but a [2 + 4] adduct. This adduct is

(7) (a) Fukui, K. *J. Phys. Chem.* **1970**, *74*, 4161. (b) Gonzalez, C.; Schlegel, H. B. *J. Phys. Chem.* **1989**, *90*, 2154.

(8) (a) Sauer, J.; Sustmann, R. *Angew. Chem., Int. Ed. Engl.* **1980**, *19*, 779. (b) Kistiakowsky, G. B.; Lacher, J. R. *J. Am. Chem. Soc.* **1936**, *58*, 123.

(9) The former and the latter integers stand for numbers of π electrons of butadiene and acrolein participating in the present cycloadditions, respectively.

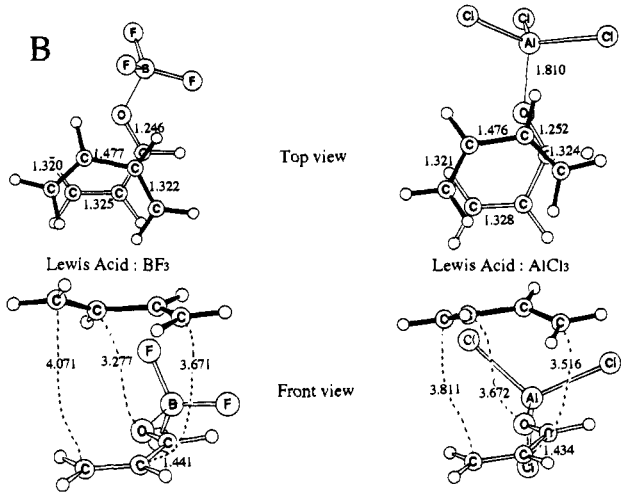

Figure 4. Geometries of weakly interacting systems composed of butadiene and Lewis acid-coordinated acrolein. The large capital "**B**" will be used in Figure 6 and Scheme 2.

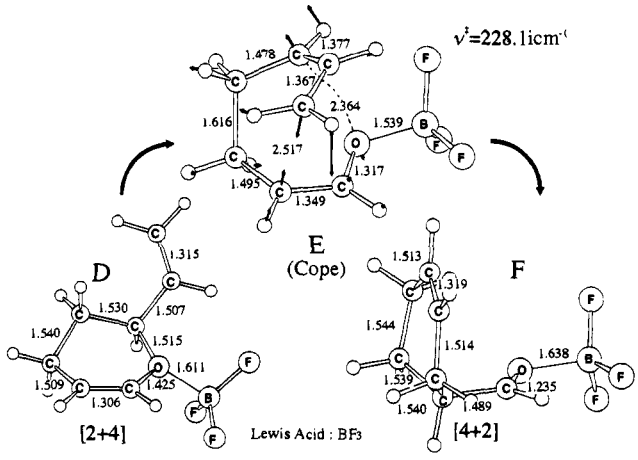

Figure 5. Geometries of two cycloadducts, [2 + 4] and [4 + 2], and their isomerization transition state optimized with RHF/3-21G. Three large capitals, **D**, **E**, and **F**, will be used in Figure 6 and Scheme 2.

shown as **D** in Figure 5. The endo addition path with BF_3 is for the [2 + 4] adduct, vinyldihydropyran. This adduct is not experimentally detected,[4a] but our calculations predict that, under the reaction condition, it should be isomerized to the final product.

The transition state of the isomerization is shown as **E** in Figure 5. This is a (3,3) sigmatropic (i.e., Cope or Claisen, called here Cope) rearrangement. This Diels–Alder reaction involving a Cope rearrangement is unprecedented. IRC calculation starting from the Cope transition state confirms the presence of the [2 + 4] adduct **D** at the end of IRC. The final product **F** has been obtained at the other end of IRC. Scheme 2 presents the computed stepwise endo path.

We used IRC calculations to determine whether the $AlCl_3$-assisted endo addition in Figure 3 leads to a [4 + 2] adduct or to a [2 + 4] adduct. While the RHF/3-21G transition state gives a [4 + 2] adduct, the RHF/6-31G* & 3-21G gives a [2 + 4] adduct. This method-dependent product demonstrates that the potential-energy surface around the region of the $AlCl_3$-containing transition state is very flat. Birney and Houk suggested, first, that the flatness leads to dual channels.[5] It is very critical for the reaction to take either the direct [4 + 2] adduct-formation path or the [2 + 4] → Cope → [4 + 2] path. This selectivity depends on the kind of Lewis acids as well as on computational methods.

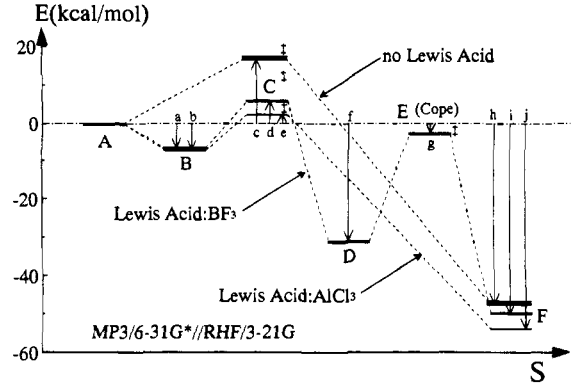

Figure 6. Three potential-energy profiles of acid-free, BF_3- and $AlCl_3$-containing Diels–Alder reactions calculated by the MP3/6-31G*//RHF/3-21G method. Stabilizing (<0) or destabilizing (>0) energies (in kcal/mol) relative to those of reactant (**A**) are as follows. For the acid-free system, $c = +16.80$, and $h = -47.45$. For BF_3, $a = -6.53$, $d = +6.09$, $f = -30.76$, $g = -2.70$, and $i = -49.68$. For $AlCl_3$, $b = -7.06$, $e = +2.64$, and $j = -53.52$.

Scheme 2

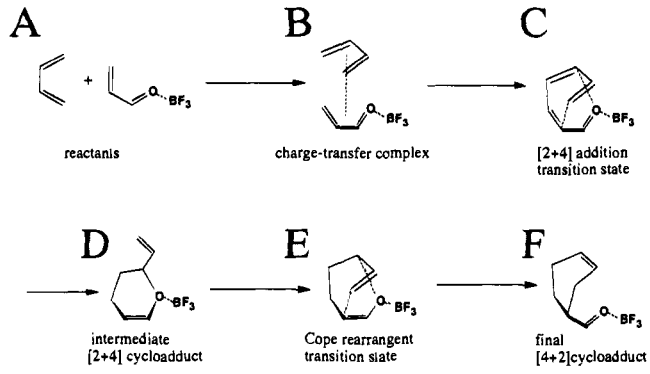

Figure 6 exhibits energy diagrams. The direct [4 + 2] adduct-formation path is taken for the reaction with $AlCl_3$. In the stepwise process with BF_3, the **B** → **C** → **D** step is confirmed to be the rate-determining step. $AlCl_3$ is found to be a stronger Lewis acid than BF_3, both kinetically and thermodynamically. $AlCl_3$ stabilizes the π–π complex, **B**, and the final product, **F**, more than BF_3 does. Also, the activation energy generated by $AlCl_3$ is smaller than that generated by BF_3.

IV. Concluding Remarks

This paper has dealt theoretically with Diels–Alder reactions uncatalyzed and catalyzed by commonly-used Lewis acids, BF_3 and $AlCl_3$. The reaction rate enhanced by Lewis acid has been clearly demonstrated by the computed activation energies. At initial stages of the acid-catalyzed additions, charge-transfer complexes (**B**'s) are formed. The geometries of these complexes reflect the FMO interaction (Scheme 3). But unfortunately the nodeless orbital overlap (*i*) does not give rise to a covalent-bond formation.[10] As the cycloaddition proceeds, the ambigious overlap (i) begins to be overcome by the left-ended one (*ii*). The growth of *ii* makes the geometry quite asymmetric and brings the electronic charges of the diene to the enolate moiety.

The upper part of Scheme 4 shows dual back charge-transfers. The weight of two canonical resonance structures determines the [4 + 2] or [2 + 4] selectivity. In the lower part of Scheme 4, a spectrum from the [4 + 2] to [2 + 4] paths is shown. The addition without Lewis acids favors [4 + 2] over [2 + 4]. The

(10) It was pointed out that the symmetric orbital interaction cannot work so importantly as the antisymmetric one in Diels–Alder reactions. See: Fujimoto, H.; Inagaki S.; Fukui K. *J. Am. Chem. Soc.* **1976**, *98*, 2670.

Scheme 3

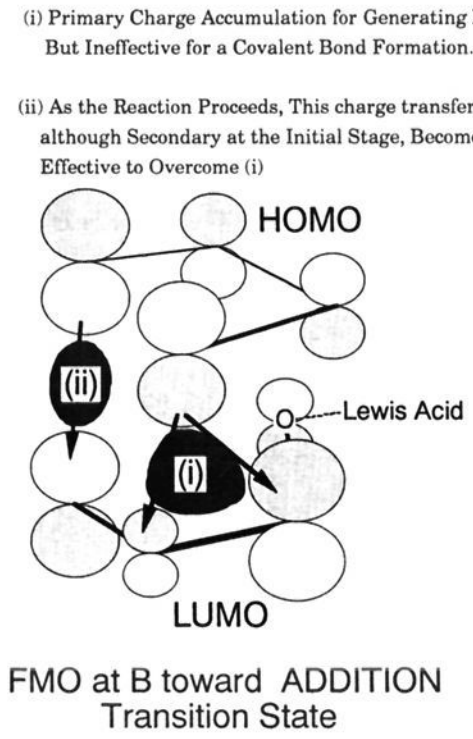

RHF/3-21G E_a of [4 + 2] is by 3.18 kcal/mol smaller than that of [2 + 4].[11] With $AlCl_3$, it cannot be judged definitely whether the addition transition state is for the [4 + 2] adduct or for the [2 + 4] one (borderline). With BF_3, the addition transition state leads to the [2 + 4] adduct followed by a Cope rearrangement toward the [4 + 2] adduct. Sometimes the [2 + 4] adduct is detected. When nitroalkenes catalyzed by $SnCl_4$ react with dienes, [2 + 4] adducts (nitronates) are obtained, not the normal-electron-demand [4 + 2] adducts.[12] These reactions belong to the BF_3 case.

Acknowledgment. The authors thank the Information Processing Center of Nara University of Education for the allotment of the CPU time of the CONVEX C-220 computer and the Computer Center of Nara University for that of the CONVEX C-3420 computer. The present work was supported in part by a Grant-in-Aid for Scientific Research on Priority Area "Theory of Chemical Reactions" from the Ministry of Education, Science and Culture. We greatly appreciate professor Swan's kindness in carefully reading the manuscript and correcting our English.

(11) For the butadiene–acrolein system, another transition state, the [2 + 4] transition state, for the formation of acid-free vinyldihydropyran has been obtained. This geometry and total energy are also included in the supporting information.

(12) Denmark, S. E.; Kesley, B. S.; Moon, Y-C. *J. Org. Chem.* **1992**, *57*, 4912.

Scheme 4

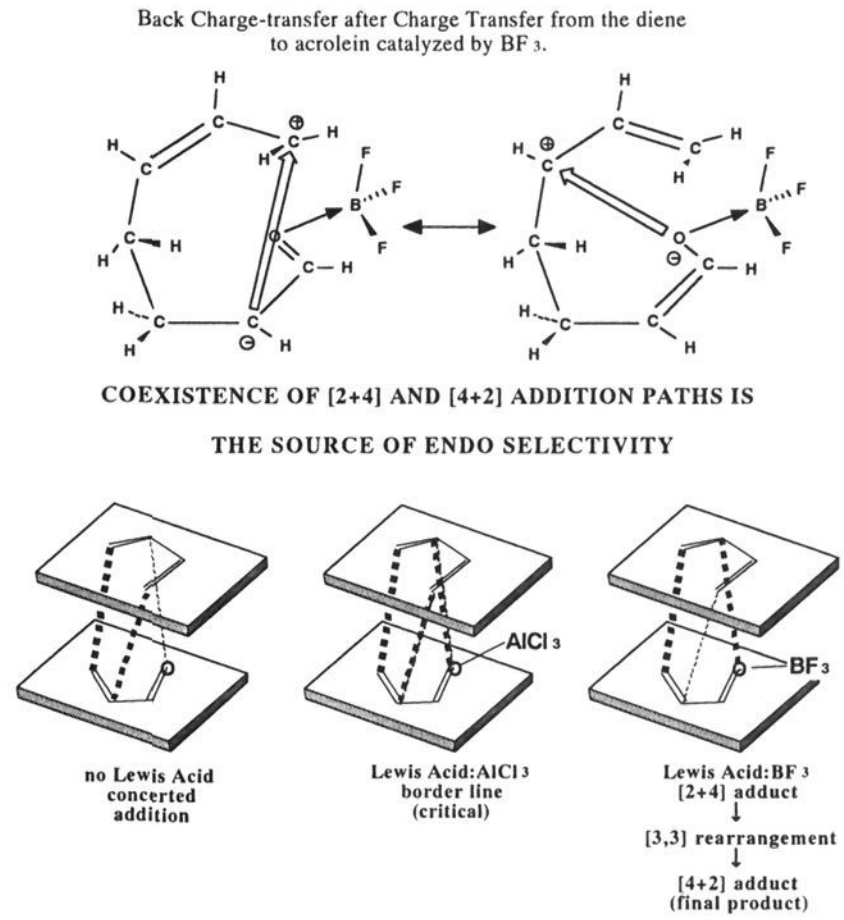

Supporting Information Available: *Z*-matrices of geometries optimized with various methods in Figures 1–6 (23 pages). This material is contained in many libraries on microfiche, immediately follows this article in the microfilm version of the journal, can be ordered from the ACS, and can be downloaded from the Internet; see any current masthead page for ordering information and Internet access instructions.

JA941283W